Available online at www.sciencedirect.com
SCIENCE DIRECT
Journal of Solid State Chemistry 179 (2006) 1330–1334
JOURNAL OF SOLID STATE CHEMISTRY
www.elsevier.com/locate/jssc

The effects of $ZnGa_2O_4$ formation on structural and optical properties of ZnO:Ga powders

Agnaldo de Souza Gonçalves*, Sergio Antonio Marques de Lima, Marian Rosaly Davolos, Selma Gutierrez Antônio, Carlos de Oliveira Paiva-Santos

Instituto de Química, Universidade Estadual Paulista—UNESP, P.O. Box 355, 14800-900 Araraquara/SP, Brazil

Received 24 November 2005; received in revised form 16 January 2006; accepted 22 January 2006
Available online 28 February 2006

Abstract

Gallium-doped zinc oxide (ZnO:Ga 1, 2, 3, 4 and 5 at%) samples were prepared in powder form by modifying the Pechini method. The formation of zinc gallate ($ZnGa_2O_4$) with the spinel crystal structure was observed even in ZnO:Ga 1 at% by X-ray diffraction. The presence of $ZnGa_2O_4$ in ZnO:Ga samples was also evidenced by luminescence spectroscopy through its blue emission at 430 nm, assigned to charge transfer between Ga^{3+} at regular octahedral symmetry and its surrounding O^{2-} ions. The amount of $ZnGa_2O_4$ increases as the dopant concentration increases, as observed by the quantitative phase analysis by the Rietveld method.

Keywords: Zinc gallate; Impurities in semiconductors; Crystal structure and symmetry; Optical properties; Doping; ZnO:Ga; $ZnGa_2O_4$; Pechini method

1. Introduction

ZnO is a nonstoichiometric oxide with the hexagonal wurtzite structure and a wide band gap (~3.3 eV). Along with remarkable optical properties, such as high refractive index, ZnO is also a green emitter. Even though the mechanism of this emission is still unclear, some light has been shed in this respect recently [1,2]. Endowed with many applications, ZnO has attracted much attention in dye-sensitized solar cells either as a porous nanostructured electrode [3] or even more recently as a nanowire anode [4]. It can also be used as a transparent conductor oxide (TCO) [5] in several optoelectronic devices. For application as TCO, the electrical conductivity of ZnO should be improved, which may be achieved by replacing Zn^{2+} ions by other ions with higher valence (acting as efficient shallow donors) such as In^{3+}, Al^{3+} and Ga^{3+} [5–7]. In gallium-doped zinc oxide (ZnO:Ga), Ga^{3+} is expected to cause a small lattice distortion due to the Zn and Ga similar tetrahedral radii, acting as an efficient shallow donor in ZnO. Unfortunately, gallium doping might give rise to spinel structures ($M^{II}Ga_2O_4$) when the matrix to be doped is ZnO, especially when heavily doped samples are taken into account. Solubility limits are reported to be close to 3 at% of Ga in ZnO [8,9]. The formation of $ZnGa_2O_4$ is likely to take place in ZnO:Ga, changing the microscopic structural and electronic environment of Ga^{3+} in the ZnO matrix. $ZnGa_2O_4$ has the normal cubic spinel crystal structure in which Zn^{2+} ions occupy tetrahedral sites and Ga^{3+} ions the octahedral ones. This compound might have interesting effects on the electrical and optical properties of ZnO:Ga since it has insulator properties, that is, a band gap of about 5 eV [10]. The formation of zinc gallate may be observed by carefully examining the X-ray diffraction (XRD) patterns of ZnO:Ga powders. Some of the most intense reflections of $ZnGa_2O_4$ might be observed, especially when dealing with heavily doped samples. The formation of $ZnGa_2O_4$ has been observed even in thin-film XRD patterns [11]. The amount of zinc gallate in ZnO:Ga may be determined by using quantitative phase analysis by the Rietveld method (RM) [12]. In this method some parameters, such as scale factor, preferred orientation, crystallite size, and microstrain are refined for the model structure until the best fit is obtained between the observed powder XRD pattern and the calculated one. In this work,

*Corresponding author. Fax: +55 16 3322 7932.
E-mail address: davolos@iq.unesp.br (A. de Souza Gonçalves).

0022-4596/$ - see front matter © 2006 Elsevier Inc. All rights reserved.
doi:10.1016/j.jssc.2006.01.046

we report on the synthesis of ZnO and ZnO:Ga 1, 2, 3, 4 and 5 at% by the modified Pechini method [13] along with the quantitative phase analysis by the RM.

2. Experimental section

Zinc acetate dihydrate (ACS-QEEL, reagent grade) was dissolved in deionized water under stirring and heating at 60 °C. Citric acid (VETEC, reagent grade) and monoethylene glycol (CHEMCO, reagent grade) were used as the monomers to form the resin. Doping was achieved by adding to the solution an appropriate amount of gallium nitrate (Aldrich, 99.9%) in the ratios Ga:Zn = 1, 2, 3, 4 and 5 at%. To achieve a homogeneous system, the Pechini method [14] was adapted by using ethylenediaminetetraacetic acid (EDTA) to the synthesis [13]. The Pechini solution obeys the molar ratio 1:3:16 of zinc citrate: citric acid: monoethylene glycol. The amount of EDTA was calculated for total metal complexation. The pH of the resulting solution was adjusted around 5.0 by adding ammonium hydroxide. By heating the mixture at about 100 °C a clear solution was achieved with a significant increase in its viscosity. The resin gave rise to fine powders after the heat treatment in air at 900 °C for 4 h. Thermogravimetric (TGA) and differential thermal analysis (DTA) of ZnO and ZnO:Ga 5 at% were carried out using a SDT 2960 simultaneous TG-DSC in the temperature range 30–1400 °C at a heating rate of 20 °C/min under an air flux. The powder samples were characterized by X-ray diffractometry, XRD, using a Rigaku RINT 2000 (copper target, $\lambda = 1.5406$ Å) at a scanning rate of 0.02°/03 s and photoluminescence (PL) spectroscopy, (Fluorolog SPEX F212 fluorescence spectrometer equipped with an R928 Hamamatsu photomultiplier). A 450 W Xe lamp was used as the excitation source in PL measurements. Emission spectra of ZnO and ZnO:Ga samples were obtained at room temperature with excitation at 370 nm. The quantitative phase analysis was achieved by using the RM and the Rietveld refinement program GSAS [15]. The $ZnGa_2O_4$ sample was prepared by the solid-state route [16] from ZnO (Baker and Adanson, reagent grade) and Ga_2O_3 (Aldrich, 99.999%). The emission spectrum of the zinc gallate sample synthesized from the solid-state route was performed at room temperature under 250 nm excitation.

3. Results and discussion

The DTA and TGA curves of pure ZnO and ZnO:Ga 5% are shown in Fig. 1.

The same behavior was observed for ZnO:Ga 1, 2, 3 and 4 at%. The TGA curves indicate a strong weight loss up to 600 °C due to the decomposition of the resin. Thus, pure and doped samples prepared by the modified Pechini method have to be heat-treated at temperatures higher than 600 °C in order to avoid the presence of organic residues. The absence of organic matter in ZnO and ZnO:Ga powders heat treated at 900 °C for 4 h was confirmed by infrared (FT-IR) spectroscopy.

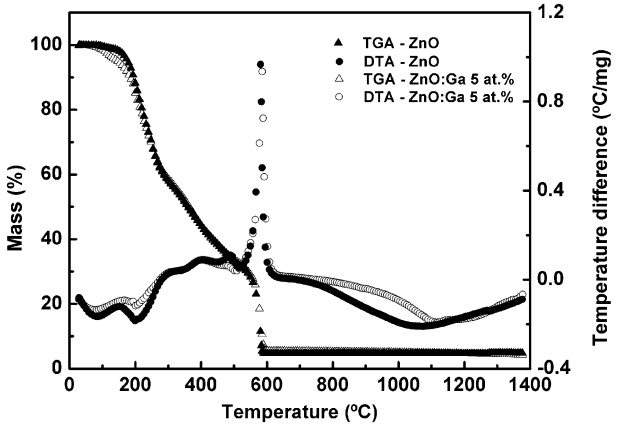

Fig. 1. Differential thermal analysis and thermogravimetric curves of ZnO and ZnO:Ga 5 at%.

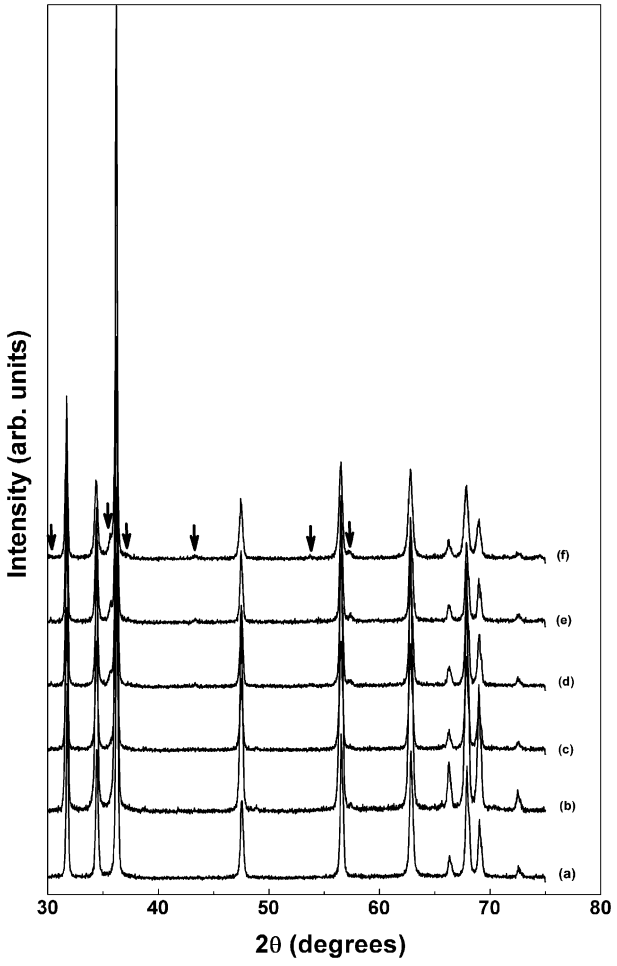

Fig. 2. Powder XRD patterns (Cu$K\alpha$ radiation) of pure and gallium-doped zinc oxide prepared by the modified Pechini method: (a) ZnO, (b) ZnO:Ga 1 at%, (c) ZnO:Ga 2 at%, (d) ZnO:Ga 3 at%, (e) ZnO:Ga 4 at% and (f) ZnO:Ga 5 at%. Some observed reflections associated to $ZnGa_2O_4$ are marked with arrows.

The powder XRD patterns of pure and gallium-doped zinc oxide are shown in Fig. 2. All samples (ZnO and

ZnO:Ga) have the zincite structure (JCPDS 14-3651). It is observed that all gallium-doped zinc oxide samples present also the cubic spinel crystal structure of $ZnGa_2O_4$ (JCPDS 38-1240). This may be observed by carefully examining the powder XRD patterns of ZnO:Ga with Ga:Zn ratios higher than 2 at%. The most intense peaks of zinc gallate (related to the 311, 511 and 440 reflections) are clearly observed in the powder XRD patterns of ZnO:Ga 3–5 at%, and they were used in the refinements by the RM to determine the amount of $ZnGa_2O_4$ in ZnO:Ga samples. Some expected reflections related to zinc gallate are: ~30.3° (220), ~35.7° (311), ~37.3° (222), ~43.4° (400), ~53.8° (422), ~ 57.4° (511) and ~63.0° (440) as indicated with arrows in Fig. 2.

One of the most intense peaks (the 3 1 1 reflection) of zinc gallate with the spinel cubic crystal structure may be observed in Fig. 3.

Besides the substitutional sites with tetrahedral symmetry in which gallium ions substitute for zinc ions, in this work the formation of $ZnGa_2O_4$ indicates that an additional kind of gallium sites is available in gallium-doped zinc oxide samples: the non-substitutional sites with octahedral symmetry which come from the spinel crystal structure of $ZnGa_2O_4$. The presence of two classes of gallium sites was revealed by means of NMR spin-echo shape measurements in all samples investigated containing 2 at% Ga [8]. The first class of gallium sites was assigned to substitutional gallium (a narrow NMR line) since they exhibited shift and relaxation properties dominated by the local hyperfine fields of conduction electrons [8]. The second class of gallium sites presented a broad NMR line (that is, a substantial quadrupolar broadening due to lattice distortion) and a low relaxation rate, indicating a distorted gallium site with essentially no coupling to the conduction electrons [8]. In this work we suggest that this second class of gallium sites might be due to the presence of some $ZnGa_2O_4$ in ZnO:Ga samples. These non-substitutional sites in which gallium ions occupy octahedral symmetry have no coupling to conduction electrons essentially in view of the wide band gap of zinc gallate ($\cong$5.0 eV). The octahedral symmetry of gallium ions depends on the atmosphere in which $ZnGa_2O_4$ was heat-treated. In a reducing atmosphere there is the formation of oxygen vacancies (V_o^*) at tetrahedral or octahedral sites [17]. These V_o^* defects of the O_h site distort the octahedral symmetry [18]. The resulting non-substitutional gallium site will then be distorted depending on the atmosphere in which zinc gallate was formed.

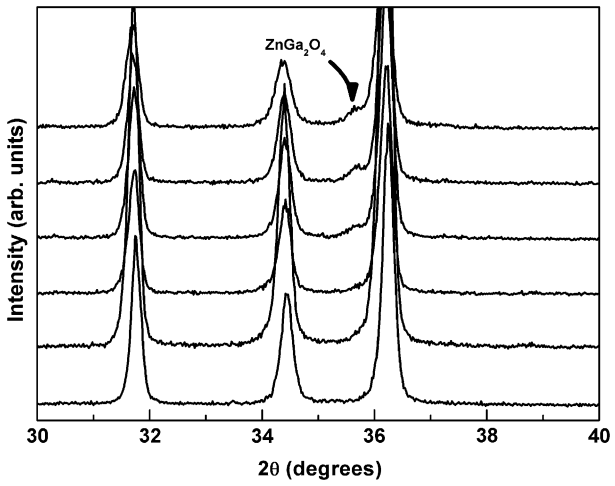

Fig. 3. Zoomed powder X-ray diffraction patterns of pure and gallium-doped zinc oxide samples.

The refined structural parameters from powder X-ray Rietveld analysis are shown in Table 1.

The S indexes (goodness of fit) of all the refinements were lower than 1.5, showing good convergence. From the quantitative phase analysis by the RM it is observed that the amount of $ZnGa_2O_4$ increases as the dopant concentration increases. The behavior of the a and c unit-cell parameters of the hexagonal zincite structure under increasing dopant level is difficult to establish due to the formation of $ZnGa_2O_4$.

The excitation spectra of ZnO and ZnO:Ga samples show a band around 370 nm related to electron transition from valence to conduction band. The excitation spectrum at room temperature of ZnO:Ga 4 at% is shown in Fig. 4.

The emission spectra of pure and gallium-doped zinc oxide are shown in Fig. 5.

The visible emission of ZnO has recently been assigned to a transition of a photogenerated electron from the conduction band edge (or from a shallow level close to it) to a trap level [2]. The emission spectra show a broad band around 530 nm for ZnO and 550 nm for gallium-doped zinc

Table 1
Refined structural parameters of pure and gallium-doped zinc oxide samples

% of gallium	Cell parameters (Å)		R_{wp}	R_{Bragg}	% of zincite (in weight)	% of $ZnGa_2O_4$ (in weight)
	a	c				
0	3.24947 (2)	5.20495 (6)	9.71	5.26	100	0
1	3.25147 (2)	5.20417 (5)	9.83	4.11	99.030 (3)	0.0970 (4)
2	3.25123 (2)	5.20417 (5)	10.76	4.30	99.327 (2)	0.67 (3)
3	3.25127 (2)	5.20437 (5)	8.78	4.82	96.878 (7)	3.12 (5)
4	3.25074 (2)	5.20405 (5)	8.96	6.39	96.696 (8)	3.30 (4)
5	3.251047 (2)	5.20498 (5)	9.61	6.76	92.68 (3)	7.02 (7)

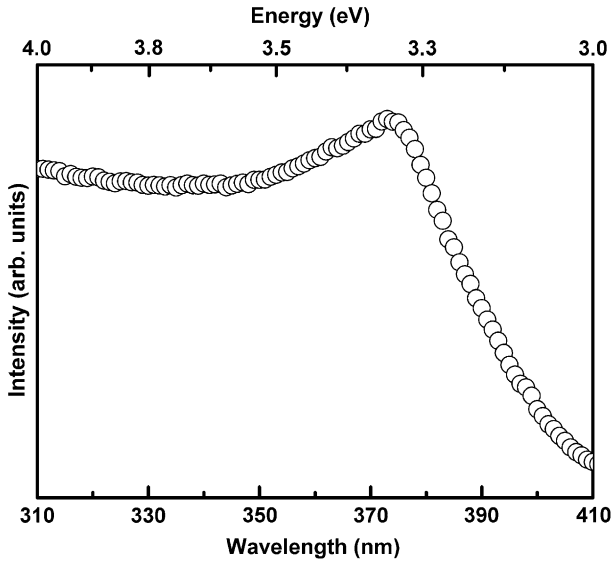

Fig. 4. Excitation spectrum ($\lambda_{em} = 550$ nm) of ZnO:Ga 4 at% obtained at room temperature.

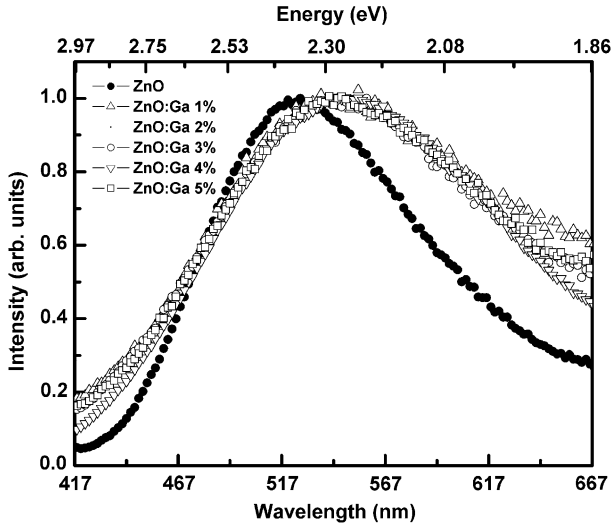

Fig. 5. Emission spectra ($\lambda_{exc} = 370$ nm) of ZnO and ZnO:Ga obtained at room temperature.

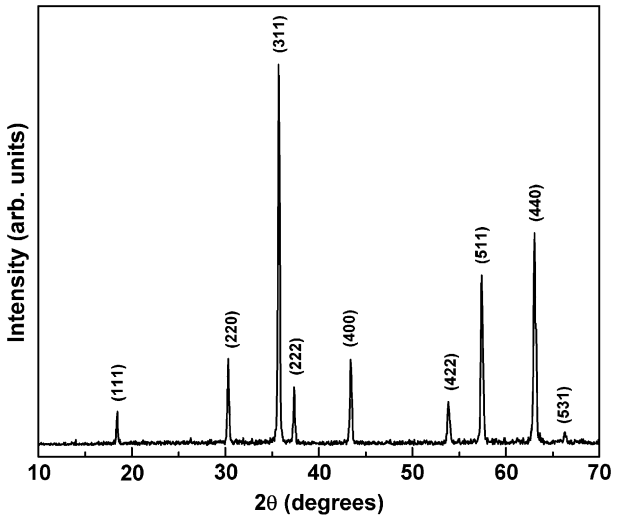

Fig. 6. Powder XRD pattern (Cu$K\alpha$ radiation) of zinc gallate prepared by the solid-state route.

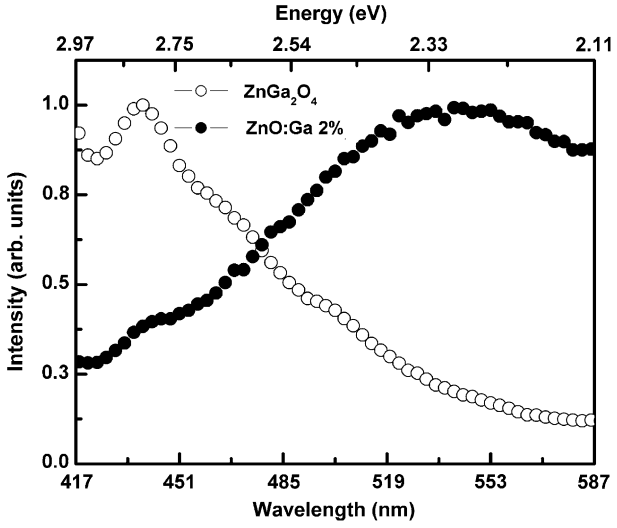

Fig. 7. Emission spectra of ZnO:Ga 2 at% and $ZnGa_2O_4$ obtained at room temperature.

oxide. The observed redshift in the emission spectra of gallium-doped zinc oxide samples is expected since Ga^{3+} acts as a shallow donor impurity in ZnO. A new band is formed close to the conduction band edge of ZnO in ZnO:Ga, which decreases the energetic difference between the shallow levels near the conduction band and the levels associated with oxygen vacancies, the possible recombination centers for the visible emission of ZnO [1,2]. The band broadening around 430 nm is probably related to an emission in the blue region ($\cong$2.9 eV), which is the characteristic emission color of zinc gallate [17]. Zinc gallate was then synthesized by the solid-state route in order to investigate its luminescence properties. The powder XRD pattern of $ZnGa_2O_4$ is shown in Fig. 6.

From the powder XRD pattern in Fig. 6 only zinc gallate with the spinel structure is observed.

The emission spectra of ZnO:Ga 2 at% (under excitation at 370 nm) and zinc gallate prepared by the solid-state route (under excitation at 250 nm) are shown in Fig. 7 for comparison.

The broadening around 430 nm in the emission spectrum of ZnO:Ga 2 at% is probably related to the emission of zinc gallate due to charge transfer between Ga^{3+} ions at regular octahedral symmetry and its O^{2-} ligands [19]. It is interesting to note that the $ZnGa_2O_4$ formed in ZnO:Ga 2 at% shows a low-intensity blue emission under 370 nm excitation instead of usually ~250 nm [17,18]. Since ZnO:Ga 2 at% was heat-treated in a slightly reducing atmosphere due to the burning of organic matter, the zinc gallate formed might have some of the octahedral sites

distorted by the presence of V_o^* defects. This distortion gives rise to two emission bands for zinc gallate: the 360 nm emission (originating from Ga–O transition) and the 680 nm emission (usually assigned to the transition from the V_o^* state to the O^{2-} state) [17]. The excitation at 370 nm for $ZnGa_2O_4$ present in ZnO:Ga 2 at% might involve states liable for the ultraviolet emission which after radiative decay turns into blue emission. This blue emission under 370 nm excitation of $ZnGa_2O_4$ present in ZnO:Ga 2 at% is related to a distorted gallium site into the spinel structure, the second class of gallium sites in ZnO:Ga discussed previously.

The formation of $ZnGa_2O_4$, observed in the XRD patterns of ZnO:Ga powders and quantified by quantitative phase analysis by using the RM, was also optically detected by PL spectroscopy. It is important to note that even though Zn^{2+} ions still occupy tetrahedral sites in the normal spinel cubic structure of $ZnGa_2O_4$, Ga^{3+} ions occupy octahedral sites instead of tetrahedral sites when doping the zincite structure of ZnO. This structural change, along with the wider band gap of $ZnGa_2O_4$, might help explain the electrical and optical properties of heavily doped samples of ZnO:Ga. Besides, some light is shed into the microscopic structure and electronic surroundings of metal impurities in ZnO.

4. Conclusions

The Pechini method was adapted by using EDTA in order to obtain gallium-doped zinc oxide in the homogeneous system. It was observed that all gallium-doped zinc oxide samples present the hexagonal wurtzite structure and also the spinel crystal structure of zinc gallate. The amount of zinc gallate present in ZnO:Ga increases under increasing dopant concentration. The formation of $ZnGa_2O_4$ in ZnO:Ga powders, observed by powder XRD, was also evidenced by PL spectroscopy. The presence of zinc gallate in gallium-doped zinc oxide samples has structural and optical effects on the optoelectronic properties of ZnO:Ga since it gives rise to non-substitutional gallium sites.

Acknowledgments

Financial support by FAPESP is gratefully acknowledged. ASG thanks FAPESP for the scholarship and M.A. Cebim for helpful discussions. The authors also thank F.L. Fertonani and E.Y. Ionashiro for performing the TG measurements.

References

[1] A. van Dijken, E.A. Meulenkamp, D. Vanmaekelbergh, A. Meijerink, J. Lumin. 87–89 (2000) 454.
[2] A. van Dijken, E.A. Meulenkamp, D. Vanmaekelbergh, A. Meijerink, J. Lumin. 90 (2000) 123.
[3] K. Keis, C. Bauer, G. Boschloo, A. Hagfeldt, K. Westermark, H. Rensmo, H. Siegbahn, J. Photochem. Photobiol. A 148 (2002) 57.
[4] M. Law, L.E. Greene, J.C. Johnson, R. Saykally, P.D. Yang, Nat. Mater. 4 (2005) 455.
[5] K.Y. Cheong, N. Muti, S.R. Ramanan, Thin Solid Films 410 (2002) 142.
[6] V. Assunção, E. Fortunato, A. Marques, A. Gonçalves, I. Ferreira, H. Águas, R. Martins, Thin Solid Films 442 (2003) 102.
[7] E. Fortunato, A. Gonçalves, V. Assunção, A. Marques, H. Águas, L. Pereira, I. Ferreira, R. Martins, Thin Solid Films 442 (2003) 121.
[8] N. Roberts, R.P. Wang, A.W. Sleight, W.W. Warren Jr., Phys. Rev. B: Condens. Matter Mater. Phys. 57 (1998) 5734.
[9] R.P. Wang, A.W. Sleight, D. Cleary, Chem. Mater. 8 (1996) 433.
[10] T. Omata, N. Ueda, K. Ueda, H. Kawazoe, Appl. Phys. Lett. 64 (1994) 1077.
[11] J.J. Robbins, C. Fry, C.A. Wolden, J. Cryst. Growth 263 (2004) 283.
[12] H.M. Rietveld, J. Appl. Crystallogr. 2 (1969) 65.
[13] A.S. Gonçalves, S.A.M. Lima, M.R. Davolos, Eclet. Quim. 27 (2002) 293.
[14] M.P.U. Pechini, US Patent 3.330.697, 1967.
[15] C.O. Paiva-Santos, A.A. Cavalheiro, M.A. Zaghete, M. Cilense, J.A. Varela, M.T.S. Giotto, Y.P. Mascarenhas, Adv. X-ray Anal. 44 (2001) 38.
[16] S.K. Sampath, J.F. Cordaro, J. Am. Ceram. Soc. 81 (1998) 649.
[17] J.S. Kim, H.I. Kang, W.N. Kim, J.I. Kim, J.C. Choi, H.L. Park, G.C. Kim, Y.H. Hwang, S.I. Mho, M.C. Jung, M. Han, Appl. Phys. Lett. 82 (2003) 2029.
[18] J.S. Kim, H.L. Park, C.M. Chon, H.S. Moon, T.W. Kim, Solid State Commun. 129 (2004) 163.
[19] T.K. Jeong, H.L. Park, S.I. Mho, Solid State Commun. 105 (1998) 105.